CERN/SPSC/78-95
SPSC/P 110/S
17 August 1978

STUDY OF π^-p INTERACTIONS WITH NEUTRAL FINAL STATES

IHEP[1]-IISN[2]-LAPP[3] Collaboration

F.G. Binon[2], C. Bricman[2], Yu.B. Bushnin[1], V.A. Davidov[1], S.V. Donskov[1], J. Dufournaud[3], M. Gouanère[3], A.V. Inyakin[1], D.T. Jayanti[2], V.A. Kachanov[1], D.B. Kakauridze[1], G.V. Khaustov[1], A.V. Kulik[1], J.P. Lagnaux[2], A.A. Lednev[1], Yu.V. Mikhailov[1], J.P. Peigneux[3], Yu.D. Prokoshkin[1], R. Roosen[2], S.A. Sadovsky[1], V.A. Senko[1], D. Sillou[3], M. Spighel[3], A.V. Starzev[1], J.P. Stroot[2], A.N. Sytin[1]

In the present experiment it is proposed to study the production of neutral particles or states decaying into photons in the reaction $\pi^- + p \rightarrow M^0 + n$ at SPS energies.

Special attention is paid to the measurement of the production of heavy particles with hidden quantum numbers and of possible new heavy spinless states decaying into two photons.

The large four-momentum transfer behaviour of binary processes involving known neutral mesons and the production of new meson resonances with high mass and spin are also being studied. Complex multiparticle final states will be analysed as a by-product.

The central unit of the experimental set-up is a 4000 cell Čerenkov hodoscope spectrometer (GAMS) which allows the measurement of the momentum vector of each gamma in a multigamma event.

The longitudinal position of the interaction point in the liquid hydrogen target is measured by the Čerenkov light intensity.

A guard system, made of scintillation counters and lead-glass Čerenkov counters, is used to trigger on neutral events (triggers).

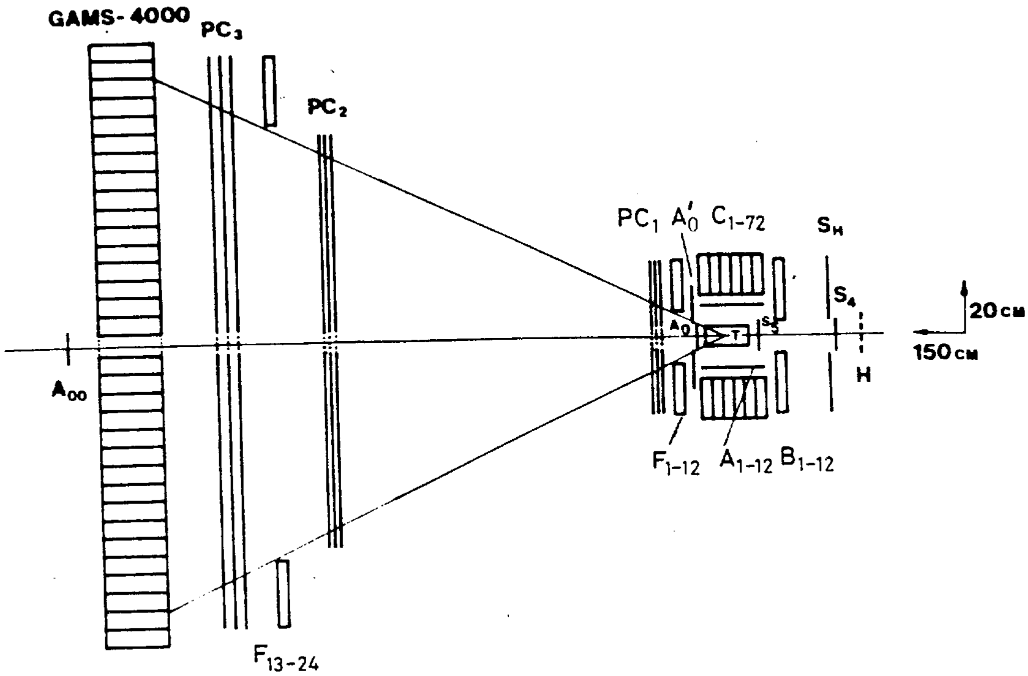

Experimental set-up

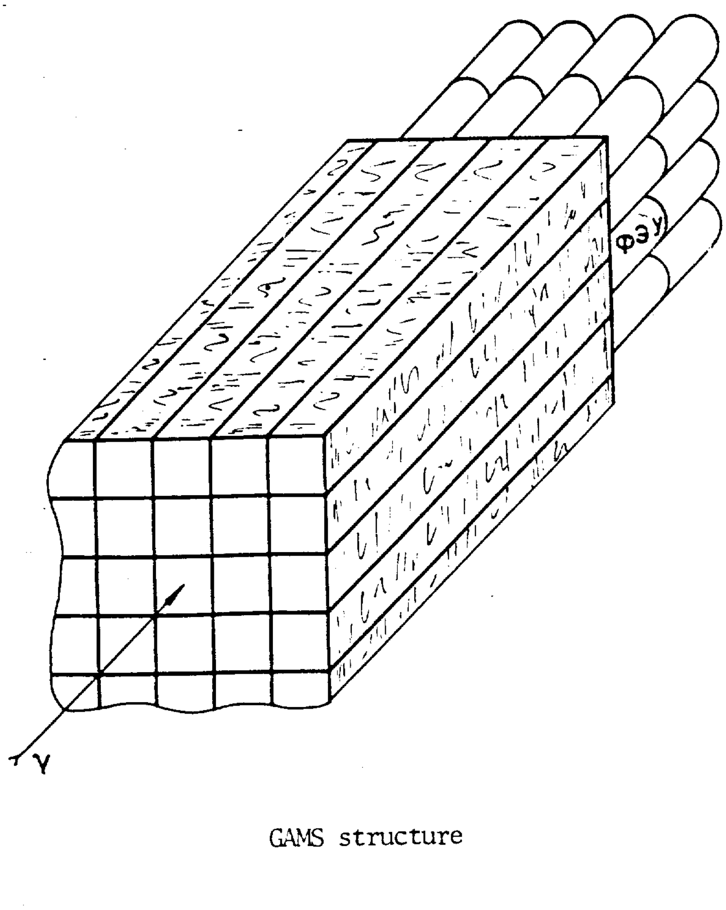

GAMS structure

EUROPEAN ORGANIZATION FOR NUCLEAR RESEARCH

CERN/SPSC/78-95
SPSC/P 110
17 August 1978

PROPOSAL

STUDY OF $\pi^- p$ INTERACTIONS WITH NEUTRAL FINAL STATES

IHEP[1] - IISN[2] - LAPP[3] Collaboration

F.G. Binon[2], C. Bricman[2], Yu.B. Bushnin[1], V.A. Davidov[1], S.V. Donskov[1], J. Dufournaud[3], M. Gouanère[3], A.V. Inyakin[1], D.T. Jayanti[2], V.A. Kachanov[1], D.B. Kakauridze[1], G.V. Khaustov[1], A.V. Kulik[1], J.P. Lagnaux[2], A.A. Lednev[1], Yu.V. Mikhailov[1], J.P. Peigneux[3], Yu.D. Prokoshkin[1], R. Roosen[2], S.A. Sadovsky[1], V.A. Senko[1], D. Sillou[3], M. Spighel[3], A.V. Starzev[1], J.P. Stroot[2] and A.N. Sytin[1]

GENEVA
1978

1) Institute for High-Energy Physics, Serpukhov, USSR.
2) Institut Interuniversitaire des Sciences Nucléaires, Bruxelles, Belgium.
3) Laboratoire d'Annecy de physique des particules, France.

CONTENTS

1. INTRODUCTION

A characteristic feature of strong interactions at high energy is the production of a large number of secondary particles. The multiplicity of secondaries is about ten in $\pi^- p$ collisions at 300 GeV. Of these, about four are neutral on the average. Heavy resonances, which may be produced at this high energy, also have a tendency to decay through many-body channels and contribute to this multiplicity. Therefore an effective study of particle interactions in this energy region requires the use of experimental devices able to separate and to register simultaneously a large number of particles in the final state. In particular, the special class of reactions with neutral final states which decay eventually to γ-rays may now be more thoroughly studied with the newly developed multigamma spectrometer GAMS. This experimental technique has been developed at IHEP since 1973; the principle of the spectrometer and its characteristics have been tested in particle beams at the 70 GeV accelerator[1,2].

The GAMS spectrometer allows the simultaneous measurement of the coordinates and energies of a large number of photons and the reconstruction, with high accuracy, of the masses and momenta of the decaying particles[2-4]. The spectrometer can operate directly in high-intensity beams. No magnet is needed in the set-up. The advantage of this method is the possibility to detect events with a complicated topology with a very compact set-up, and to cover effectively a major part of the phase space available to the reactions under study. The set-up includes a limited number of additional detectors used for triggering and calibration purposes.

The present proposal is to study at SPS energies binary reactions with neutral final states of the type

$$\pi^- + p \rightarrow M^0 + n , \qquad (1)$$

where M^0 stands for neutral particles or states decaying finally into photons and where n is a neutron.

This will allow data to be gathered on:

i) the production of heavy particles with hidden quantum numbers like charmonium or objects composed of heavier quarks;

ii) the large four-momentum transfer behaviour of binary processes involving known mesons, which is expected to exhibit a universal t-dependence;

iii) new meson resonances with high mass and spin.

All these processes are measured simultaneously with the same experimental set-up.

In the following section is given a short description of the GAMS spectrometer and of its main characteristics. Next, the physics program is described, including the study of known processes as well as the search for new particles. In Section 4 the planning, the status of preparation, and the expected schedule for performing the experiment, are discussed.

2. EXPERIMENTAL SET-UP

The experimental set-up is shown in Fig. 1. The central unit GAMS-4000 [1,2] is a Čerenkov hodoscope spectrometer. With it are measured the energy and the impact of each gamma in multigamma states. This, together with the knowledge of the origin of the interaction, allows the determination of the mass and of the momentum vector of these states. No magnetic field is being used.

2.1 GAMS-4000

a) Detectors

GAMS-4000 is a matrix of 64 × 64 parallelepipedal lead-glass cells (Fig. 2). The Čerenkov light is detected by a photomultiplier at the end of each cell.

The main parameter of such a detector is the lateral dimension of the cell (2Δ). If, as usual, Δ is rather larger than b, the effective width of the electromagnetic showers, the coordinates of the photon or electron impact on the spectrometer can be measured only roughly, the accuracy being of the order of the half cell dimension in Fig. 3. On the other hand, if Δ is similar or smaller than b ($\lesssim$ 2 cm in F-8 glass), the shower spreads over a few cells. Comparing the amount of light in the different cells allows the determination of the gamma (or electron) coordinate to an accuracy of $\sim$ 1 mm [2,3]. Studies have been made with a model in an electron beam (Fig. 4). This spatial resolution is close to that which has been obtained with the 648-channel NICE spectrometer in experiments at Serpukhov. NICE[5,6] and also the 140-channel Cal. Tech.[7] spectrometer, which are sandwiches of scintillator strips and iron (or lead) sheets, are limited in their scope at high energies because only a limited number of simultaneously produced γ-rays, i.e. up to four, can be analysed owing to the overlap of the different projections of the showers.

GAMS is free from these shortcomings because the vector momentum of each γ is measured separately, as showers overlap at very high multiplicities only (Fig. 5). GAMS is thus well suited to the analysis of events with many gamma-rays.

The GAMS power of discrimination between very close γ-ray showers has been demonstrated experimentally[4]. Pairs of γ-rays from π^0 decay cannot be confused with a single γ-ray when their lateral separation is $\gtrsim$ 2.5 cm, i.e. even in the case when both gammas fall in the same cell of the spectrometer.

Also, an effective discrimination between hadronic and electromagnetic showers is obtained in GAMS by taking into account the difference in their respective transverse dimensions[4] (Fig. 6).

Another advantage of GAMS over other types of actually known coordinate and energy measuring spectrometers is the high time resolution of the instrument ($\sim$ 100 times faster than argon calorimeters, $\sim$ 10 times faster than MWPC γ-detectors).

b) Parameters and characteristics

- lead-glass cell dimensions	:	$38 \times 38 \times 450$ mm^3
- type of glass	:	F-8
- total number of cells	:	4096
- working area and weight of the spectrometer	:	5 m^2, 10 t
- photomultiplier	:	FEU-84-3
- accuracy in measuring photon coordinate		
at 25 GeV	:	± 2 mm
at 200 GeV	:	± 1 mm
- photon energy resolution		
at 25 GeV	:	$\pm 2.5\%$
at 200 GeV	:	$\pm 1.5\%$
- mass resolution for decaying particles	:	a few %
- time resolution	:	40 nsec gate
- number of accepted events	:	up to 1000/sec
- beam intensity	:	up to 3×10^7/sec.

GAMS energy resolution may be expressed by the formula

$$\Delta E/E \text{ (FWHM)} = 0.025 + \frac{0.13}{\sqrt{E \text{ (GeV)}}} , \tag{2}$$

as shown by existing measurements (Fig. 7).

The linearity has been studied with electrons at different energies between 1.8 and 40 GeV by the GAMS group at IHEP and between 1 and 4 GeV by the EHS group at CERN. No deviation larger than 1% has been observed (Fig. 8).

c) Electronics

The pulse-height analysis of each photomultiplier signal is made in parallel by individual ADCs organized in a modular way. The dynamical range of each ADC spans more than 4000 channels (12 bits). The maximum conversion time is 150 μsec.

Fast processing performs immediate pedestal subtraction and energy normalization (with coefficients from calibration runs). A wired preprocessor allows a determination of the effective mass, the total energy and the transverse momentum of the multigamma system being registered. This is done by evaluating the first and second moments of the signals in each cell relative to the axis of the spectrometer. In this way, a preselection of rare events can be done in presence of a huge flux of information before recording on magnetic tape (slow trigger). Taking into account the coding times, the system allows the recording of more than 500 events/sec with a multiplicity of $\sim$ 300 cells ($\sim$ 10 γ-rays).

d) Calibration

Each cell is first calibrated with defocused electron and muon beams which irradiate the spectrometer sector by sector. This method has been checked in a model at IHEP beams. A movable platform allows displacement of the 10 ton detector across the beam. The first calibration at SPS should last a week at most; the next ones could go much faster. For calibration purposes, the rate of events can be increased up to 3000 per second.

The gain of each counter is monitored through pulses from light emitting diodes. Such monitoring has also been checked to guarantee a 10^{-2} long-term stability.

2.2 Pion beam and target

For the proposed experiment a negative pion beam with an intensity of up to 3×10^7 π^-/sec will be used. One millimetre step scintillation hodoscopes define the transverse coordinates of the pions incident on the target.

The liquid hydrogen target is 60 cm long. The intensity of the Čerenkov light emitted by the beam particles in the target is measured[8]. It allows evaluation of the longitudinal coordinate of the vertex of neutral final state interactions with an accuracy of 5 cm.

2.3 Trigger

Beam particles which do not come out of the target, and which are not accompanied either by the emission of one or more charged particles or by photons emitted at large angles, give unambiguous trigger signals for the study of reaction (1). The target is completely surrounded by thin scintillation counters which detect the emission of charged particles. This guard system is completed by TF-5 lead-glass Čerenkov counters which are also surrounding the target except for the solid angle subtended by GAMS. The guard system has been designed according to the experience gained during experiments with the spectrometer NICE[9-11].

2.4 Data analysis

Methods to determine shower coordinates have been studied experimentally and are described in an earlier work[3]. They allow the reconstruction of photon coordinates with the help of logarithmic formulae convenient for on-line data handling {see Fig. 4 where the coordinates are determined experimentally through the ratio of the amplitudes of the signals detected in adjacent cells of the spectrometer: $x_B = \Delta - b \ln \frac{1}{2}[(A_i/A_{i+1}) + 1]$}. By fitting the showers, the accuracy can still be improved by a factor of 1.5 [3].

The data-handling system (shower recognition and kinematical reconstruction of the events) makes use of the experience gained with previous hodoscopic spectrometers[7,9,10].

3. PHYSICS

3.1 Study of heavy particles with hidden quantum numbers, produced in charge-exchange binary reactions

One of the key questions of present-day elementary particle physics is the study of recently discovered heavy hadrons assumed to be made of new quarks. "Pure" states with hidden quantum numbers, like $(c\bar{c})$, $(b\bar{b})$, etc., are particularly interesting.

Vector particles of such a type are much more easily studied in e^+e^- collisions than in hadron collisions where a huge background is present owing to the large number of other reactions. However, for the production of mesons with hidden flavours, having quantum numbers different from those of the photon, hadron collisions are fully competitive (as, for example, the production of spin 0 mesons, which are obtained in e^+e^- collisions only through the decay of vector mesons). This kind of study allows verification of predictions of QCD.

Charge exchange reactions of type (1), with subsequent decay into two photons,

$$\pi^- + p \to X + n \qquad (3)$$
$$\hookrightarrow 2\gamma$$

will be studied with GAMS in order to obtain information on even spin particles with hidden charm c or beauty b and other possible states with analogous quark structure.

In spite of its low yield, reaction (3) has two attractive features. Firstly, a quark-antiquark system $(u\bar{u}, d\bar{d})$ is formed in the final state which may later annihilate into states $(c\bar{c})$, $(b\bar{b})$, or others, via two gluons. Secondly, the branching ratio of the decay $X \to 2\gamma$ is rather high for particles with such a large mass: $BR(X \to 2\gamma) \sim 2Q^2(\alpha/\alpha_s)$ where α_s is the gluon-quark coupling constant, Q is the quark charge, i.e. $BR \sim 2 \times 10^{-3}$. Experimental data give a value $BR \gtrsim 7 \times 10^{-3}$ for X(2.85).

The first information on reaction (3) with hadronic production of X(2.85), which is probably the lowest pseudoscalar state of charmonium η_c, was obtained in the fourth joint CERN-IHEP experiment[12]. It shows that for this particular reaction $\sigma \times BR(X \to 2\gamma) \simeq 2 \times 10^{-34}$ cm^2 at 40 GeV/c. When the beam momentum increases, the cross-section should not drop rapidly ($\sim 1/p$). This gives the possibility to study X(2.85) production in reaction (3) at the highest energies available at the SPS where the experimental conditions become considerably better. Firstly, the mass resolution of the GAMS spectrometer improves when the energy rises and reaches $\Delta M \simeq 50$ GeV (half height) in the mass region around ~ 3 GeV for a beam momentum $\gtrsim 150$ GeV/c. Secondly, the detection efficiency (and thus also the suppression efficiency) of background processes improves with energy. An estimate, based on experimental data[12], shows that a background level $\lesssim 10^{-37}$ cm^2 can be reached. Altogether one expects to detect ~ 300 X(2.85) and $\chi(3.4)$ in a one month period*) of SPS running with a background of less than 10%.

The lowest pseudoscalar member η_b of the Υ family could also be observed in reaction (3) in spite of its very large mass (~ 9 GeV). The branching ratio for $\eta_b \to 2\gamma$ is only four times smaller than that for $\eta_c \to 2\gamma$ ($Q_b = 1/3$ in the formula above) and the production cross-section decreases with mass like $\sim M^{-3}$ (or M^{-2} in the case of a threshold enhancement). So, one may hope to detect ~ 10 decays $\eta_b \to 2\gamma$ during the experiment. One should notice that this measurement is free of background. Previous experience shows that the background level is expected to be less than 10^{-38} cm^2 for such heavy masses (extrapolation of Ref. 12 data).

More generally, the GAMS spectrometer allows the search for states decaying into two photons with masses up to ~ 12 GeV.

The above considerations have been limited essentially to processes in which "the present new" particles are produced. However, one should remark that, just as measurements of muon pairs happened to be a good way to discover narrow vector particles of a new kind, precise studies of γ pairs with heavy masses could give the possibility to find new spinless particles, for which a characteristic signature is two-photon decay.

3.2 Study of binary charge-exchange reactions at large four-momentum transfers

Recently, binary charge-exchange reactions producing neutral mesons have been intensively studied in the region of small and medium four-momentum transfers $|t| \lesssim 1$ (GeV/c)^2. These studies have shown that such reactions are in reasonable

*) Numbers of events quoted here and below correspond to one "ideal" month of data taking with the following assumptions: the SPS delivers $\sim 10^4$ bursts/day and the intensity of the beam is 3×10^7 π^-/burst, i.e. $\sim 10^{13}$ π^-/month. There will be $\sim 6 \times 10^{11}$ interacting π^-/month in a 60 cm long liquid H_2 target.

agreement with the predictions of Regge models: the forward diffractive cone is shrinking with increasing incident pion energy; the differential cross-sections decrease exponentially with increasing $|t|$ and are well described using linear Regge trajectories.

The large $|t|$ region of reactions (1) has remained largely unexplored because of the very small cross-sections at high energies. This region is interesting as a break has been observed[10] in the exponential behaviour of the differential cross-sections (see Fig. 9). The t-dependence of the cross-section is found to be similar for processes which are very different from the point of view of t-channel exchange, such as $\pi^- p \to \eta n$ (A_2 exchange), $\pi^- p \to \omega n$ (ρ and B exchange) and $pp \to pp$ (Pomeron exchange), which shows that this fact is not fortuitous. In the same t-region the behaviour of the effective trajectory also suddenly changes. This is seen clearly in Fig. 10, where the A_2 trajectory as obtained from data on the reaction $\pi^- p \to \eta n$ is displayed. The break in the Regge trajectory shows that the cross-section for $-t > 1$ $(\mathrm{GeV}/c)^2$ does not decrease with increasing energy as fast as predicted by the standard Regge model, but more like $1/p^2$. This means that cross-section measurements at large t with high statistical accuracy are possible even at the highest energies available at the SPS. Theoretical models to explain this behaviour are being developed at the present time [see, for example, Schrempp and Schrempp[13]].

Practically, the cross-sections of type (1) reactions are measured simultaneously with a set-up whose geometry changes rather little. The geometry is determined by the spatial resolution of the spectrometer (it is necessary to detect efficiently neutral pions), on the one hand, and by the t interval to be covered, on the other hand. The proposed spectrometer allows coverage of a $-t$ interval up to 20 $(\mathrm{GeV}/c)^2$ in the case where $M^0 = \pi^0$. This interval shrinks when the mass of M^0 increases [8 $(\mathrm{GeV}/c)^2$ for a mass of 1 GeV]. However, this is not a real drawback as evidently the limitation due to the small counting rate dominates for larger $|t|$.

Below are listed some reactions that can be studied and expected results are discussed.

One of the most studied reactions of type (1) today is

$$\pi^- + p \to \eta + n \,. \qquad \eta \hookrightarrow 2\gamma \tag{4}$$

To evaluate its differential cross-section at large $|t|$, a model[13] has been used which describes rather well existing data and according to which the cross-section oscillates going through successive minima separated by steps of $2\pi/R \approx 1$ GeV/c in the $\sqrt{-t}$ scale, $R \simeq 10^{-13}$ cm being the universal hadron radius. Another model, without oscillations, but with cross-sections diminishing exponentially, has also been used. The results are shown in Fig. 11 together with the limits reached in preceding experiments and the expected cross-sections to be measured with GAMS-4000 during one month of data taking at 300 GeV/c. The NICE experiment has shown that the principal source of background at large $|t|$ is inelastic processes in which the system M^0 is produced with a large effective mass and decays into a η and one (or more) extra neutral pion(s). At 40 GeV/c this background amounted to 10^{-35} $cm^2/(GeV/c)^2$ in the region $-t \geq 3$ $(GeV/c)^2$. The high resolution of the GAMS spectrometer and, particularly, its ability to register simultaneously a large number of photons allows identification and elimination of this background (which is an interesting subject by itself; cf. Section 3.3) at a level lower than 10^{-36} $cm^2/(GeV/c)^2$.

The reaction

$$\pi^- + p \rightarrow \eta' + n \qquad \eta' \hookrightarrow \gamma \tag{5}$$

will be studied at a level of accuracy quite different from before. It is also going through A_2 exchange (if both η and η' are members of the same pseudoscalar meson nonet, as is now generally accepted). Until recently only a few hundred events of this rare process had been observed at high energies[14]. More than 10,000 events could be gathered in the present experiment. This would allow observation of the break in the t-dependence of the cross-section, if it exists.

Evidently, data on the charge-exchange reaction

$$\pi^- + p \rightarrow \pi^0 + n \tag{6}$$

at large $|t|$ will be simultaneously collected. The statistics will be more than one order of magnitude larger than in previous FNAL and IHEP experiments and the second maximum in the cross-sections will be studied thoroughly (Fig. 12). The position of the minimum around $t \simeq -0.55$ $(GeV/c)^2$ will be obtained with high precision and this will allow observation of whether it moves with energy. The behaviour of the ρ trajectory at large $-t$ will also be obtained.

Final states with more complex topologies than just two photons will also be studied. For example:

a) The reaction

$$\pi^- + p \rightarrow \omega + n \qquad \omega \hookrightarrow \pi^0\gamma \tag{7}$$

presents great interest. It is practically the only way to study the behaviour of trajectories with unnatural spin-parity (B exchange). More than 10,000 events could be collected with GAMS-4000 up to $-t = 3\ (\mathrm{GeV}/c)^2$ allowing the test of universality of the change in the t-dependence of the cross-section for $-t \gtrsim 1\ (\mathrm{GeV}/c)^2$ (cf. Fig. 9).

b) The production of the h(2020) meson with $J^{PC} = 4^{++}$

$$\pi^- + p \to h + n \qquad \qquad (8)$$
$$\hookrightarrow \pi^0\pi^0$$

is practically unexplored. Measurements with the GAMS-4000 spectrometer would allow more than 10,000 h mesons to be produced in reaction (8) at different energies and determination of the energy dependence of its cross-section for $-t \leq 1.5\ (\mathrm{GeV}/c)^2$. The detection efficiency for this reaction is near to one over the whole phase space except for the small angular region $\cos\theta_{GJ} \simeq 1$ (Fig. 13). For the other reactions already mentioned before, which have final states with simpler topologies, the conditions of measurements are still more favourable. A hundred thousand events of reaction (1) with f meson production could be studied at the same time in a $-t$ range up to $3\ (\mathrm{GeV}/c)^2$ and at different energies.

c) The study of the reaction

$$\pi^- + p \to \phi + n \qquad \qquad (9)$$
$$\hookrightarrow \eta\gamma$$

has a great interest as the ϕ has a quark structure analogous to that of J/ψ. Though the cross-section of this reaction is greatly reduced by the Zweig rule, 1,000 ϕ's could be collected in this experiment and the dependence of the cross-section on energy and on t could be determined. Data on this reaction are missing at high energies.

d) Amongst other possible type (1) reactions, the following one

$$\pi^- + p \to A_2^0 + n \qquad \qquad (10)$$
$$\hookrightarrow \eta\pi^0$$

could also be observed. High-energy data on this reaction are scarce.

3.3 Study of the production of high-spin heavy mesons

Another part of the GAMS-4000 program is the search, in type (1) reactions, for heavy neutral mesons with large spins which subsequently decay into lighter mesons and ultimately into photons. Particularly interesting is the search for dimeson states $M^0 \to \pi^0\pi^0$ and $\eta\pi^0$.

Earlier experiments with the NICE hodoscope spectrometer permitted the discovery of the spin 4 meson h(2020), decaying into $\pi^0\pi^0$ [9]. The decay channel $h \to K^+K^-$ has also been observed[15]. More recently, the A_2' meson with a mass of 1900 MeV and $I^G = 1^-$, partner of the h meson in the same 4^{++} nonet, has been discovered at the CERN PS[16].

The search for members of the J = 6 and 8 nonets will be made through the study of $\pi^0\pi^0$ systems. Two facts facilitate this search: a) the dipion production cross-section appears to decrease not too fast when the mass M^0 increases and b) one does not expect a fast decrease of the $BR(M^0 \to \pi^0\pi^0)$ for masses up to 3 GeV, according to the available data on the ρ, f, g, and h mesons. In the one-pion exchange model, which is used here for estimation purposes, the cross-section of reaction (1) is given by

$$\sigma \sim m \times (2J + 1) \times BR(M^0 \to \pi^0\pi^0)\Gamma(M^0 \to all) \ ,$$

where m and J are the mass and the spin of the meson M^0, respectively. Since the width $\Gamma(M^0 \to all)$ is almost the same for all known dipions, the above expression allows us to evaluate $\sigma \times BR(M^0 \to \pi^0\pi^0)$ relatively to another particle taken as reference, e.g. the f meson. According to the spin-mass relation (Fig. 14) one expects a mass of 2530 MeV for the $J^P = 6^+$ meson and a mass of 2900 MeV for the $J^P = 8^+$ meson. The latter is probably the highest meson accessible in this experiment according to an evaluation with the preceding formula and to the estimated $\pi^0\pi^0$ continuum[9].

Large spin resonances are identified by their characteristic decay angular distribution. Reaction (1) going largely through one-pion exchange, the nearly complete spin alignment of the M^0 particles makes their spin determination easier (Fig. 15). The requirement on the spectrometer resolution increases with the spin and, since $\Delta \cos \theta_{GJ} \approx 2\ E/E \approx 1/\sqrt{E}$, the higher the spin the higher the energy at which one should work. Spin 4 particles are best observed between 80 and 150 GeV. For the larger spins J = 6 and 8 one has to go to the 150 to 300 GeV energy region. At these energies one is able to see the fast oscillations near $\cos \theta_{GJ} \approx 1$ which are characteristic of large spins. This is illustrated in Fig. 16 for a hypothetical spin 8^+ resonance.

The decay $M^0 \to \eta\pi^0$ will be studied in a similar way in order to search for high spin resonances with $I^G = 1^-$. The probability of this decay mode is expected to be rather important and the background to be comparatively small. As previous experiments have shown, the production cross-section of a $\eta\pi^0$ system with a mass higher than 1.5 GeV is 25 times less than for a $\pi^0\pi^0$ pair. This allows, for example, the observation of the decay $A_2' \to \eta\pi^0$ even if the branching ratio $BR(A_2' \to \eta\pi^0) \approx 1\%$. One must underline the unique property of the decay into $\eta\pi^0$:

the observation of this channel and the spin determination fix all quantum numbers of the decaying meson.

3.4 By-products

Previous studies of reaction (1) were limited to a multiplicity of four γ's in the final state. A spectrometer of the GAMS type gives the possibility of studying more complicated topologies, especially as the performances of the spectrometer improve with increasing energy. Systems like $\omega\pi^0$, $3\pi^0$, $\eta\pi^0\pi^0$, $\omega\omega$, ff, and others are almost not studied. The study of such systems with many γ's in the final state becomes possible at very high energies only. This is due to the fact that spectrometers like GAMS, which measure the coordinates and the energy of photons, have an energy threshold of 1 to 2 GeV. The observation of a system like $\omega\omega \to 6\gamma$, for example, is difficult even at the highest energy available at Serpukhov as the mean γ energy is still near threshold (40 GeV/c $\gtrsim$ 7 GeV). Biases caused by the apparatus to the angular and energy distributions are very large in this case. At SPS energies, the situation considerably changes: the mean γ energy rises to $\sim$ 50 GeV and the spectrometer effectively covers most of the phase space of the reaction (Fig. 17).

The study of the system $\omega\pi^0 \to 5\gamma$ will allow information to be obtained on the reactions $\pi^-p \to B^0n$ and $\pi^-p \to g^0n$. At the same time a search for new resonances both with natural ($J^P = 5^-, 7^-, \ldots$) and unnatural ($J^P = 3^+, 5^+, \ldots$) spin parity will be performed.

The possibility to study multiparticle systems with the GAMS spectrometer is illustrated using reaction $\pi^-p \to g^0n$ as an example. Figure 18 shows the reconstruction of $\omega\pi^0$ systems generated by Monte Carlo. Real showers, measured at 25 GeV with a model of the GAMS spectrometer, were used in this simulation, after suitable energy scaling. The $\sigma \times$ BR product for this reaction at 300 GeV is about 10 nb. The background from $3\pi^0$ states, which can produce 5γ events when one low energy γ is lost, was scaled from NICE data and it was found to be less than 5×10^{-2} of the g^0 peak in Fig. 18b. Figure 19 shows the detection efficiency of GAMS at SPS energies for events with $g^0 \to \omega\pi^0$ topology.

The search for isotriplet meson states with unnatural spin parity ($J^P = 4^-$, $6^-, \ldots$) could also be undertaken through the study of more complex systems like $\eta\pi^0\pi^0 \to 6\gamma$, $\omega\omega \to 6\gamma$, etc.

J/ψ production processes have to be set apart amongst multiparticle final states. With GAMS we hope to get information about processes in which J/ψ decaying into $\eta\gamma$ are produced together with neutral mesons (including those with hidden charms as well as ordinary ones, like η).

4. SCHEDULE AND OTHER QUESTIONS

4.1 Construction and tests of the experimental set-up

All technical studies with particle beams which are needed for the construction of the GAMS spectrometer (choice of the lead-glass, choice of the elementary cell dimensions and choice of the photomultiplier type, testing the calibration system, etc.) have been concluded in 1977. The characteristics of the spectrometer and its performances have been and will be further studied in the conditions of real experiments at the Serpukhov accelerator. So, GAMS-4000 could be installed in an SPS beam in a state ready for measurements.

In order to reach this goal, the GAMS program has been divided into two main phases:

i) Construction of a working model with 200 counters, called GAMS-200 [17,18]. This spectrometer has been built and tested in the 25 GeV and 40 GeV negative beams at IHEP. It is now used there by our collaboration in an experiment devoted to the precise measurement of the charge-exchange differential cross-section at small momentum transfer. Later this model will be expanded so as to become a 1/4 copy of GAMS-4000 in its final technical version. Also the existing programs for data taking and analysis will be further developed in order to reach a high level of computing efficiency.

ii) Construction in parallel of GAMS-4000, taking into account the experience gained during the first phase. At the present time, nearly all photomultipliers and the lead-glass necessary for the complete GAMS program have been delivered. The mass production of the lead-glass counters has started. They are now produced with a precision of 50 μm on each cell dimension at a rate of 200 per month. Assembling and testing of the complete set-up, including target and guard system, will take two years. The set-up could be ready to start measurements in an SPS beam in the second half of 1980 if the project is accepted before the end of 1978.

4.2 Special requirements for this experiment

i) In order to allow a fast calibration of the system, the 10 ton detector will be mounted on a movable platform. Therefore a minimum distance of 2.7 to 2.8 m is necessary between the ground and the beam axis (as, for example, in beam H8), to permit the displacement of the whole detector across the beam. The distance between the hydrogen target and GAMS itself will be varied from 10 to 40 m according to the incident pion momentum and to the mass of the decaying states.

ii) The great number of cables (over 4000 coaxial ones) renders it very essential to have the experimental hut as close as possible to the detector (the quality of the signals would be impaired if the cables had to be made much longer than $\sim$ 50 m).

4.3 Computing time and CERN help

Data evaluation will be performed on computers belonging to IHEP, IISN and LAPP. CERN computers would be used occasionally, during the preparation of the experiment. During running periods, they would be used for data manipulation and compaction before their distribution amongst the participants. Foreseen use is of the order of 20 to 25 hours CPU. The time needed for processing a four-photon event (average topology) on a CDC 7600 class computer is 6 msec CPU time for individual shower recognition and reconstruction. Another 4 msec per event are needed for kinematical fit and histogramming. About 350 1600 bpi magnetic tapes will be recorded during a running period. Their analysis will take about 50 hours of CPU time (CDC 7600 equivalent).

Use of the CERN workshops facilities would only be asked for at the installation time for minor adjustments if needed.

Electronics pool general equipment would be asked for in case of emergency due to some failure in the available apparatus.

4.4 Potential safety risks

The potential safety risks are those connected with the use of an ordinary liquid hydrogen target (volume of liquid hydrogen $\sim$ 1.5 litre).

4.5 Beam time requested

A one month period of beam time for tuning the set-up and three one-month periods (as defined on p. 6, i.e. about 10^{+13} π^-) for data taking, separated by intervals to make preliminary analysis and to change the geometry of the experiment, are requested at 300 GeV π^- energy.

5. CONCLUSIONS

A research program which is oriented towards the study of neutral particle production processes is presented. It is essentially complementary to the existing programs at the CERN SPS and at FNAL. The progress and the development of the method and techniques of hodoscope Čerenkov spectrometers open up new possibilities for particle detection. The prospects are important at the energies available at the SPS and at still higher energies.

It should be underlined that at the time of the beginning of the measurements at the SPS the experimental program highlights of the GAMS-4000 spectrometer might somewhat shift, according to the developments of high-energy physics. The structure of the universal GAMS spectrometer allows the modification of its geometry and the insertion of the spectrometer in a large class of experiments.

The groups participating in the collaboration are supported by their institutes in making the present proposal. The necessary means to build the apparatus, to make the experiments, and to analyse the data in the frame of the proposed GAMS program, will be divided between the three institutes.

REFERENCES

1) Yu.D. Prokoshkin, On designing a universal gamma spectrometer for the experiments at the SPS, CERN/SPSC/75-52/1 70, p. 12, and IHEP, Serpukhov, 1974.

2) A.V. Inyakin et al., Results on experimental study of the hodoscope spectrometer prototype, CERN/SPSC/75-52/1 70, p. 19, and IHEP, Serpukhov, 1974.

3) G.A. Akopdjanov et al., Determination of photon coordinates in a hodoscope Cerenkov spectrometer, IHEP preprint 76-110 (1976); Nuclear Instrum. Methods 140, 441 (1977).

4) V.A. Davidov et al., Particle identification in a hodoscope Cerenkov spectrometer, IHEP preprint 76-155 (1976); Nuclear Instrum. Methods 145, 267 (1977).

5) Yu.B. Bushnin et al., The measurements of the spatial coordinates of high-energy photons with a scintillation hodoscope spectrometer, IHEP preprint 72-34 (1972); Nuclear Instrum. Methods 106, 493 (1972).

6) Yu.B. Bushnin et al., A hodoscope spectrometer for high-energy photons, IHEP preprint 74-21 (1974); Nuclear Instrum. Methods 120, 391 (1974).

7) O.I. Dahl et al., The reaction $\pi^- p \rightarrow \eta n$ at high energies, Phys. Rev. Letters 37, 80 (1976).

8) F. Sergiampietri, Active hydrogen target, Proc. Internat. Conf. on Instrumentation for High-Energy Physics, Frascati, 1973 (ed. S. Stipcich) (CNEN, Frascati, 1973), p. 430.

9) W.D. Apel et al., Observation of a spin 4 neutral meson with 2 GeV mass decaying in $\pi^0\pi^0$, Phys. Letters 57B, 398 (1975).

10) W.D. Apel et al., Reaction $\pi^- p \rightarrow \eta n$ at large momentum transfer, paper 1164 submitted to the 18th Internat. Conf. on High-Energy Physics, Tbilisi, 1976, IHEP preprint 77-38 (1977); Yad. Fizika 27, 154 (1977).

11) W.D. Apel et al., Measurements of $\pi^- p \rightarrow \pi^0 n$ at large momentum transfer, IHEP preprint 77-108 (1977); Phys. Letters 72B, 132 (1977).

12) W.D. Apel et al., Observation of a meson $X \rightarrow 2\gamma$, with mass 2.85 GeV/c^2, produced in the charge-exchange reaction $\pi^- p \rightarrow Xn$ at 40 GeV/c, IHEP preprint 77-127 (1977); Phys. Letters 72B, 500 (1978).

13) B. Schrempp and F. Schrempp, Nuclear Phys. B60, 110 (1973); Phys. Letters 70B, 88 (1977) and CERN preprint TH. 2319 (1977).

14) W.D. Apel et al., Reaction $\pi^- p \rightarrow X^0 n$, $X^0 \rightarrow 2\gamma$ at momenta 15 and 40 GeV/c, IHEP preprint 74-118 (1974); Proc. 17th Internat. Conf. on High-Energy Physics, London, 1974 (Rutherford Lab., Chilton, Didcot, 1974), paper 537 and p. I-35; Yad. Fizika 25, 561 (1977).

15) W. Blum et al., Observation of a spin 4 boson resonance at 2050 MeV, Phys. Letters 57B, 403 (1975).

16) R. Baldi et al., Observation of a spin 4, isospin 1, meson resonance, Phys. Letters 74B, 413 (1978).

17) G.A. Akopdjanov et al., Study of charge exchange reactions at small momentum transfer (Programme GAMS), IHEP preprint 77-3 (1977).

18) A.V. Inyakin et al., Pulse-height analysis of a large counter system, IHEP preprint 74-22 (1974); Nuclear Instrum. Methods 120, 385 (1974).

Figure captions

Fig. 1 : Experimental set-up: S_4, S_H, S_5 are the last scintillation counters which define the beam (upstream scintillation and Čerenkov counters are not shown). T is the liquid-hydrogen target. H is a high-resolution hodoscope. A_1-A_{12} and C_1-C_{72} are scintillation and Čerenkov counters, which constitute the lateral guard system. B_1-B_{12}, F_1-F_{24} are lead-glass guard counters. A_0, A_0', A_{00}, are scintillation counters. PC_1-PC_3 are three coordinate proportional chambers. GAMS-4000 is the 4096 channel hodoscope Čerenkov spectrometer.

Fig. 2 : Structure of the hodoscope Čerenkov spectrometer GAMS-4000.

Fig. 3 : Dependence of the coordinate error σ_x on the size of the spectrometer cell. Points are experimental results for 25 GeV/c electrons. The curve was calculated with a two-exponential shower model with uncorrelated fluctuations[3].

Fig. 4 : Measured shower coordinate X_b versus electron beam position (see formula in the text). The errors show σ_x.

Fig. 5 : A typical 300 GeV Monte Carlo $\pi^- p \to h(2020)n$, $h \to \pi^0\pi^0$ event in GAMS. The γ showers are scaled up from those measured at 25 GeV. A_{ij} are pulse heights in the cells of GAMS.

Fig. 6 : Shower dispersion D versus pulse height of a summed signal A for π^- mesons (dots) and electrons (dashed area corresponds to 70% confidence level, 95% level is shown by the surrounding ellipse). Broken lines show the interval $140 < D < 320$ mm^2, adopted for the electromagnetic shower selection.

Fig. 7 : GAMS energy resolution. The straight line is a plot of formula (2).

Fig. 8 : Spectrometer linearity. Black dots were measured at IHEP with a block of nine GAMS cells. Open circles were obtained at CERN with a block of seven EHS cells.

Fig. 9 : Differential cross-sections of binary reactions. ● and ▲ are NICE IHEP data, ×, ▼, ○ are CERN and FNAL data, broken line is BNL (30 GeV) and IHEP (45 GeV) data.

Fig. 10 : A_2 trajectory according to preliminary NICE data (black points). Other points are IHEP, 1973 (open circles) and FNAL, 1976 (crosses). The curve is hand-drawn, the straight line passes through A_2 and ρ points.

Fig. 11 : t-dependence of the differential cross-section of reaction (4). The limits show the sensitivity levels of this experiment and of previous ones. Points are the data[10], crosses are the expected cross-sections at 300 GeV. The dashed line corresponds to the model with oscillations[13]. The peaks on the t-axis show the t-resolution of the apparatus.

Fig. 12 : Values of $\sqrt{-t}\ d\sigma/dt$ versus $\sqrt{-t}$ for reactions (6) at 40 GeV/c [11] and 300 GeV/c (expected data). The slope of the tangent to the maxima determines the imaginary part of the pole trajectory in the optical impact parameter model[13].

Fig. 13 : Detection efficiency of the reaction (8) at 300 GeV/c. θ_{GJ} is the angle in the Gottfried-Jackson frame.

Fig. 14 : Spin-mass dependence for mesons. At $t < 0$, the points on the ρ and A_2 trajectories are deduced from data on reactions (4) and (6).

Fig. 15 : Distribution of $\pi^0\pi^0$ events versus $\cos\theta_{GJ}$ for the h(2020) meson[9]. The curve is calculated supposing the spin of the h meson fully aligned.

Fig. 16 : Expected $\cos\theta_{GJ}$ distribution for a spin 8^+ resonance with a mass $\simeq$ 2900 MeV, taking into account the spectrometer resolution. The continuum (dotted line) is taken as isotropic. The distribution was obtained in a Monte Carlo calculation supposing the spin of the 8^+ meson r(2900) fully aligned.

Fig. 17 : Detection efficiency for reaction (1) with a 2.5 GeV mass system $M^0 \to \omega\omega$ decaying isotropically, produced at 40 and 300 GeV/c. The spectrometer threshold is 2 GeV. The distance between the target and the spectrometer is optimized in each case.

Fig. 18 : Reconstruction of events in the reaction $\pi^- p \to g^0 n$, $g^0 \to \omega\pi^0$, $\omega \to \pi^0\gamma$ at 300 GeV/c in the GAMS spectrometer (M_{g^0} = 1.67 GeV). a) Mass spectrum of all pair combinations for five photons in the final state of the reaction. The shaded area is for the photon pairs identified as $\pi^0 \to 2\gamma$. b) Scatter plot of $\pi^0\gamma$ and $\pi^0\pi^0\gamma$

masses. Each event enters the scatter plot twice because of two possible $\pi^0\gamma$ combinations (right combination gives the ω peak, wrong one gives the continuum). The non-resonant ωn^0 contribution is neglected.

Fig. 19 : Efficiency for the reaction (1) with $M^0 = g^0$ decaying as $g^0 \rightarrow \omega\pi^0$, $\omega \rightarrow \pi^0\gamma$, at 300 GeV/c.

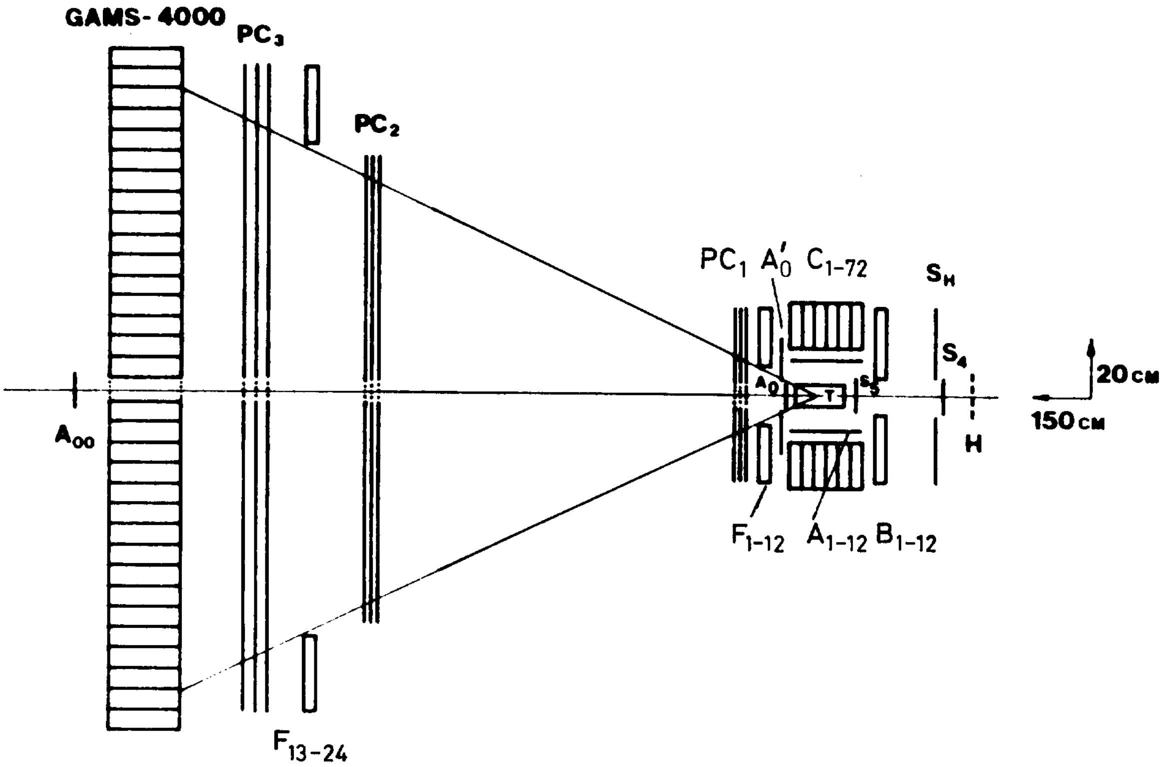

GAMS-4000
PC3
PC2
PC1
A'0
C1-72
SH
S4
20 CM
150 CM
A00
A0
T
S5
H
F1-12
A1-12
B1-12
F13-24

Fig. 1

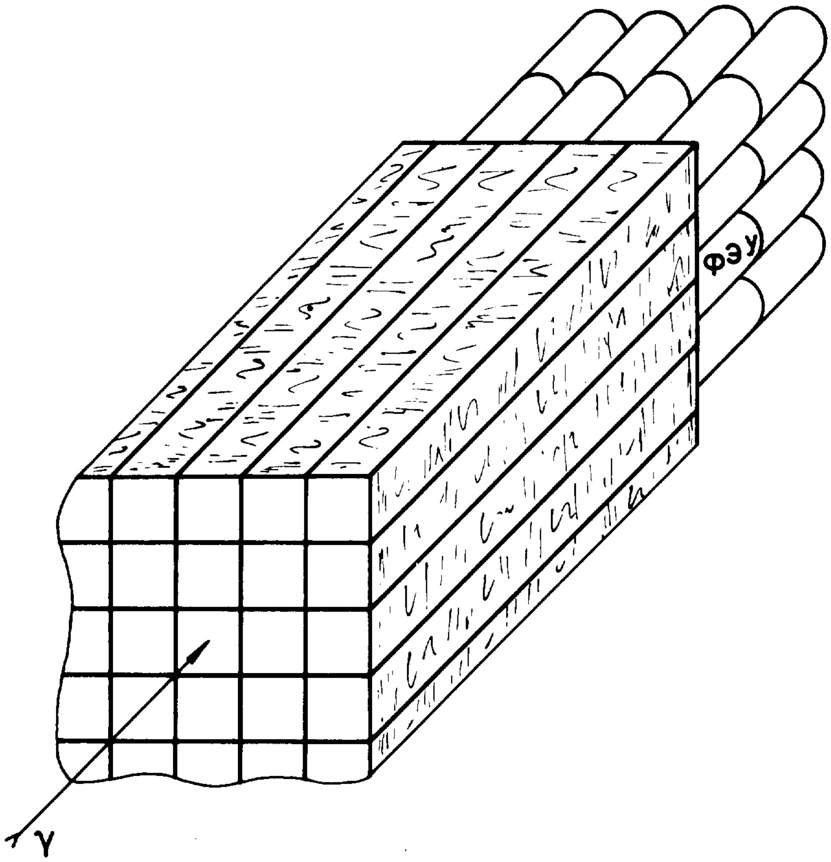

Fig. 2

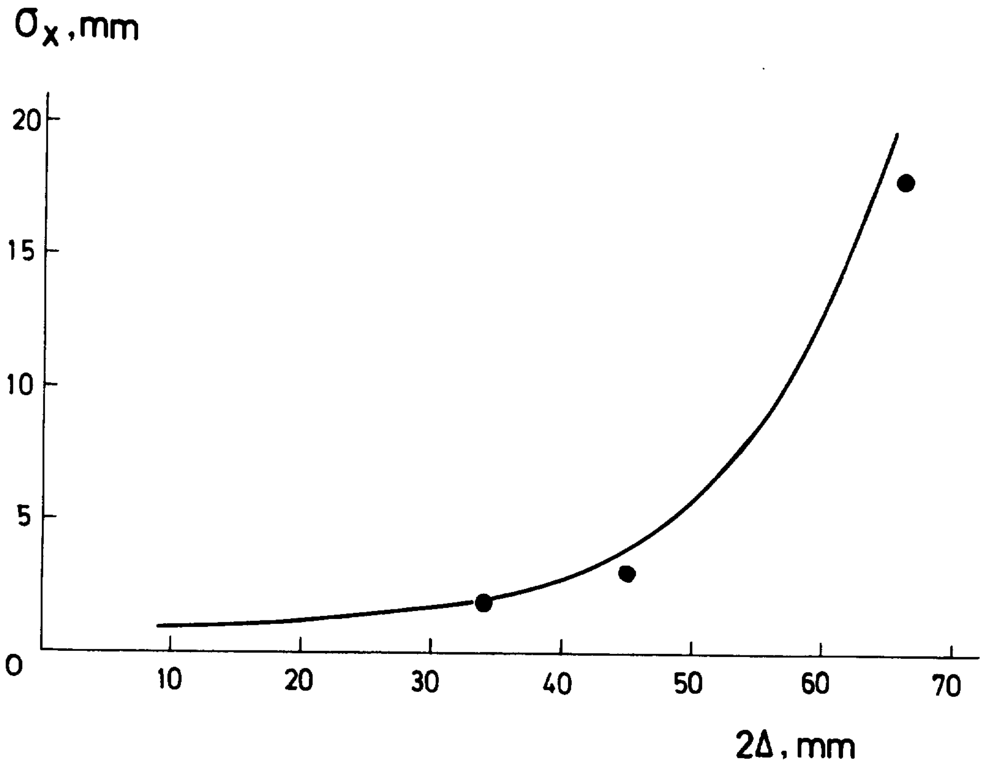

Fig. 3

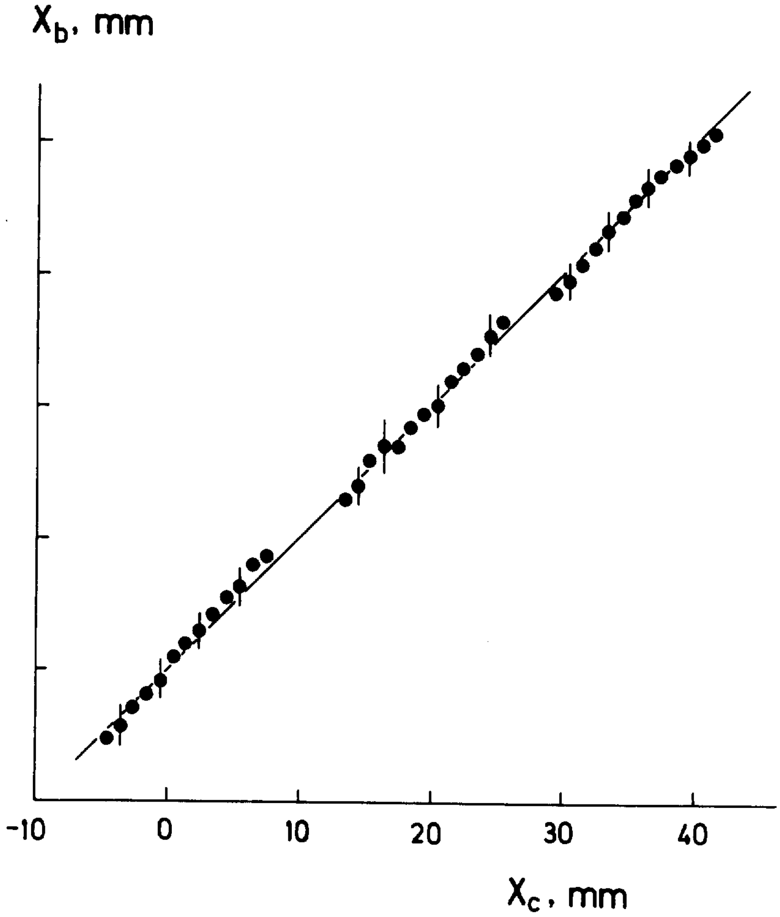

Fig. 4

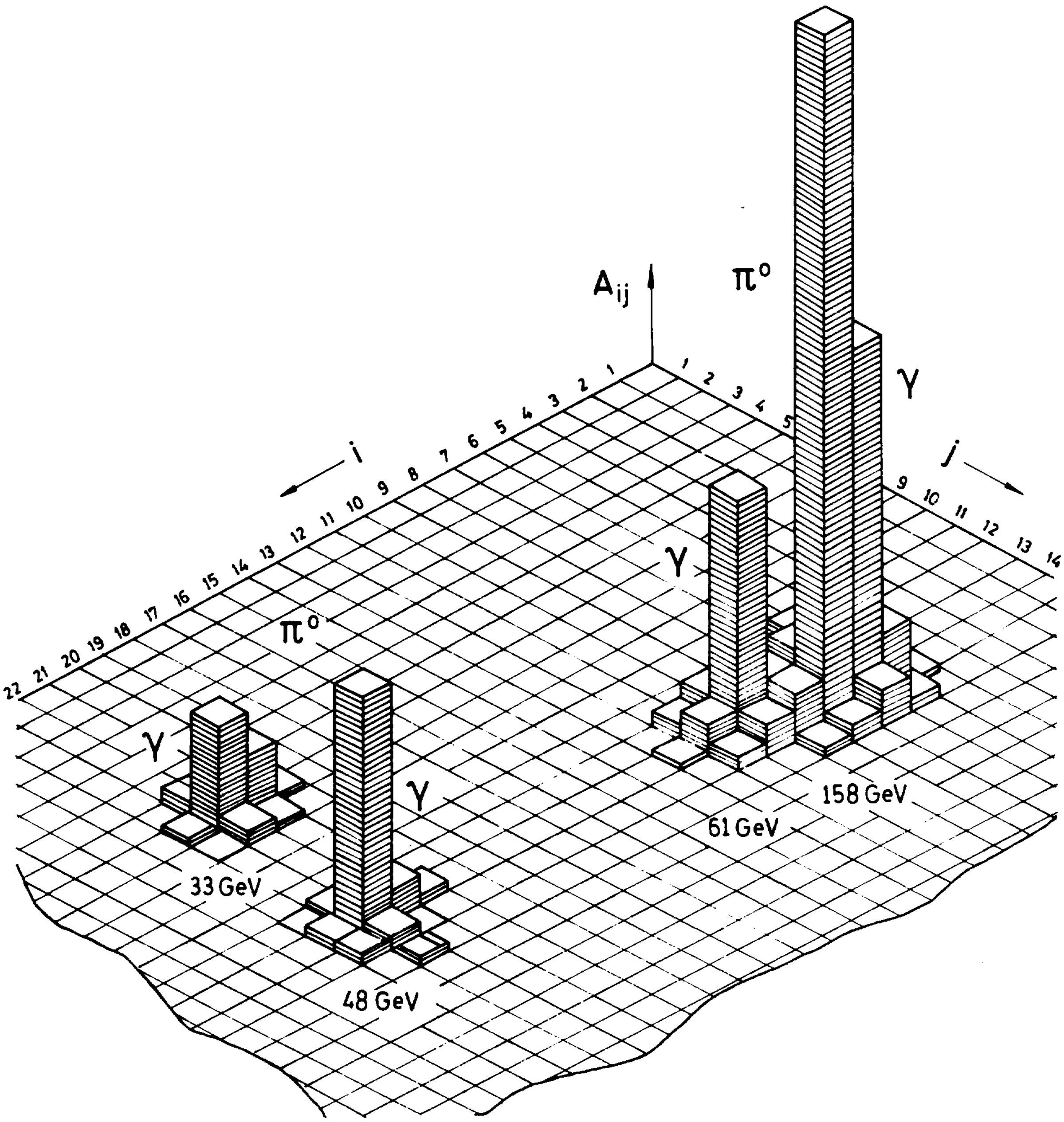

A_{ij}
π^o
γ
i
j
1 2 3 4 5 6 7 8 9 10 11 12 13 14 15 16 17 18 19 20 21 22
1 2 3 4 5
9 10 11 12 13 14
γ
π^o
γ
γ
158 GeV
61 GeV
33 GeV
48 GeV

Fig. 5

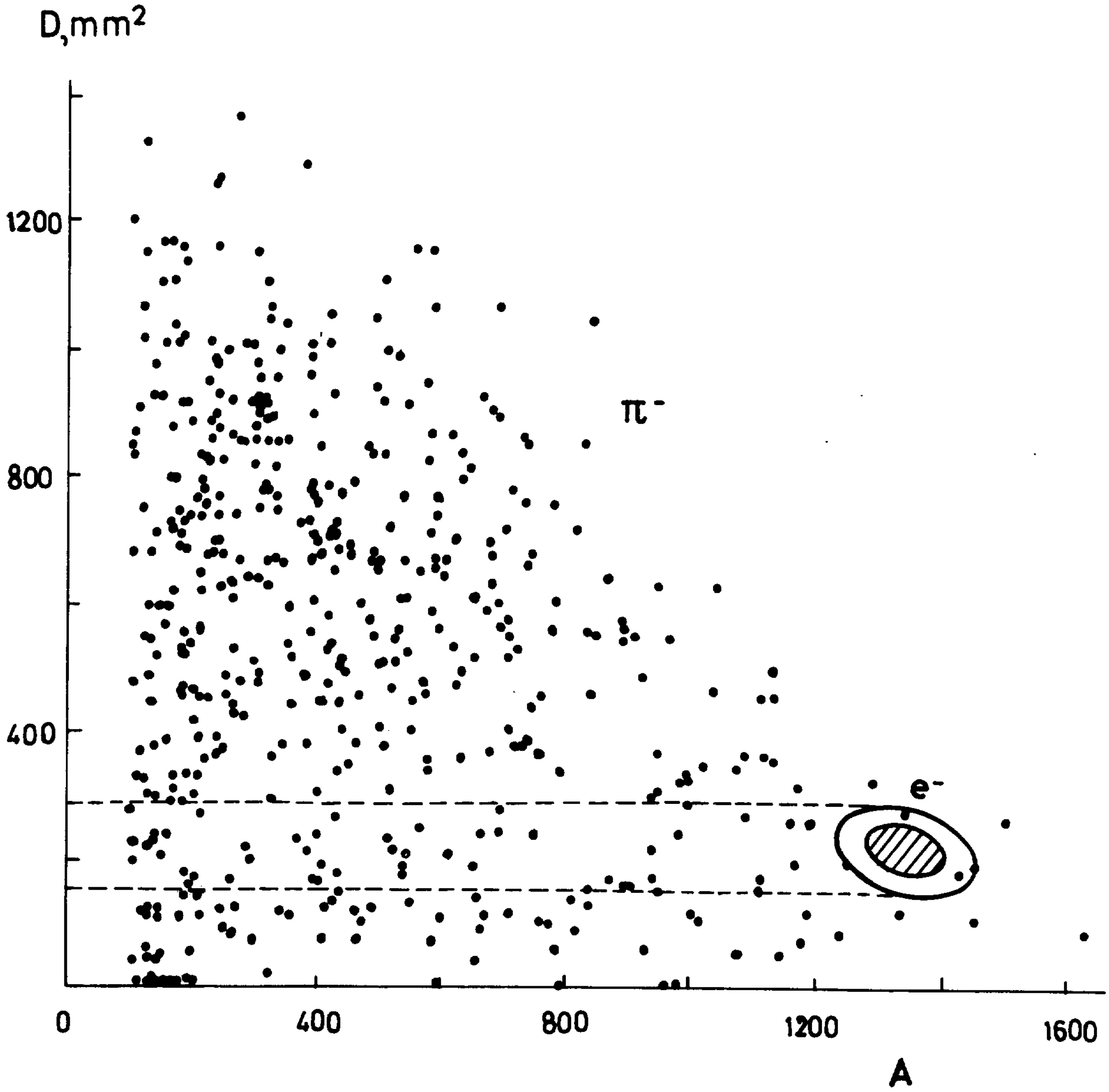

Fig. 6

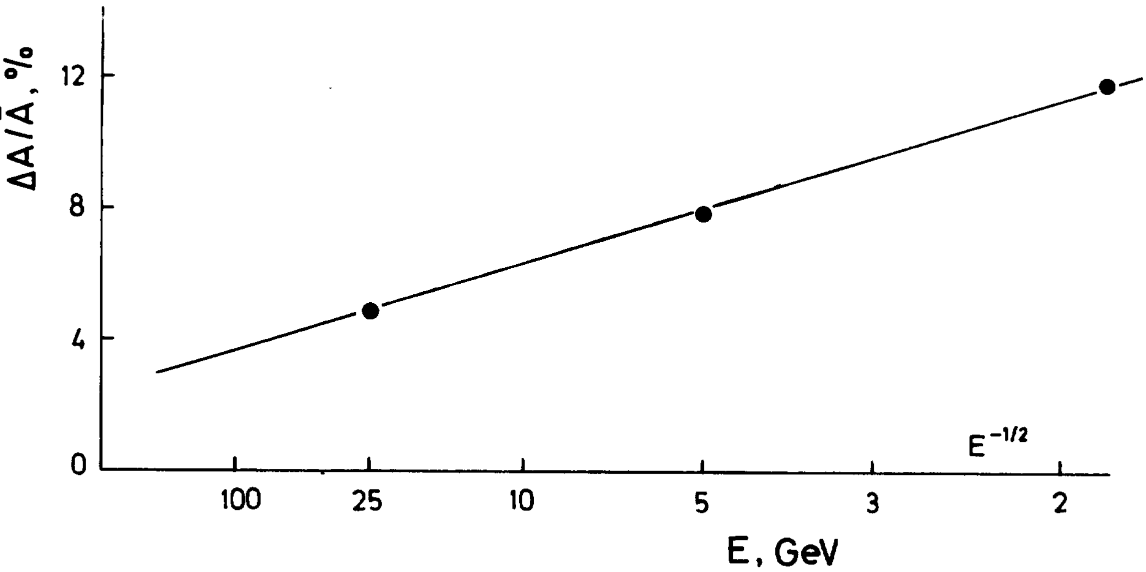

Fig. 7

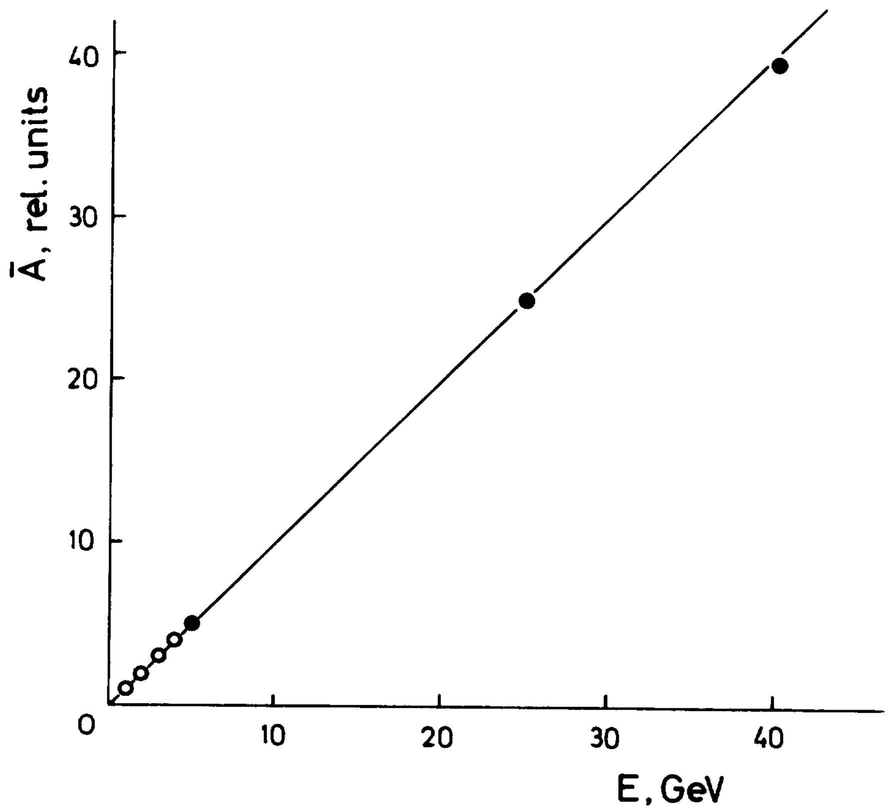

Fig. 8

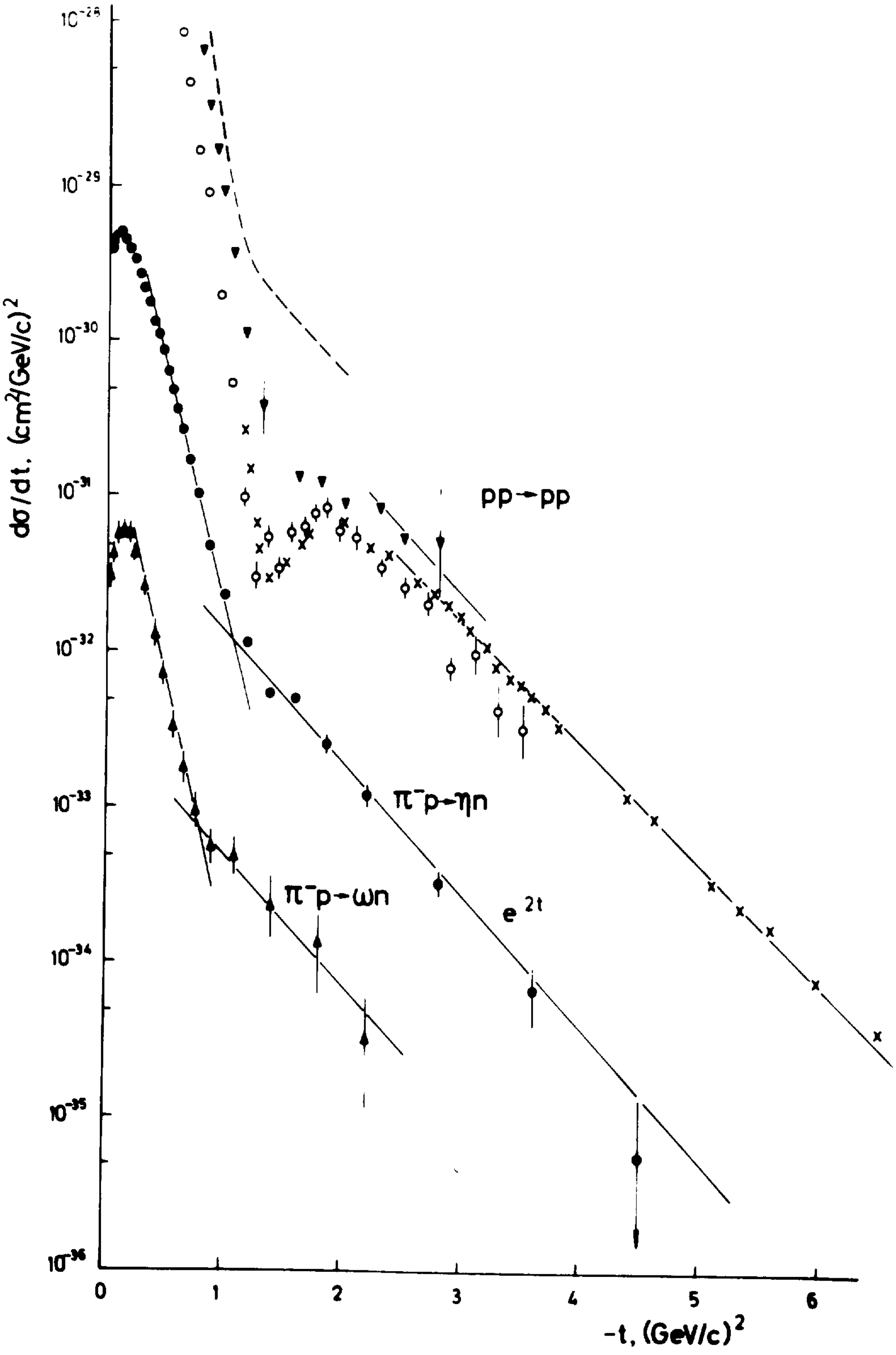

10^{-28}
10^{-29}
10^{-30}
10^{-31}
10^{-32}
10^{-33}
10^{-34}
10^{-35}
10^{-36}
$d\sigma/dt, (cm^2/GeV/c)^2$
$pp \to pp$
$\pi^- p \to \eta n$
$\pi^- p \to \omega n$
e^{2t}
0
1
2
3
4
5
6
$-t, (GeV/c)^2$

Fig. 9

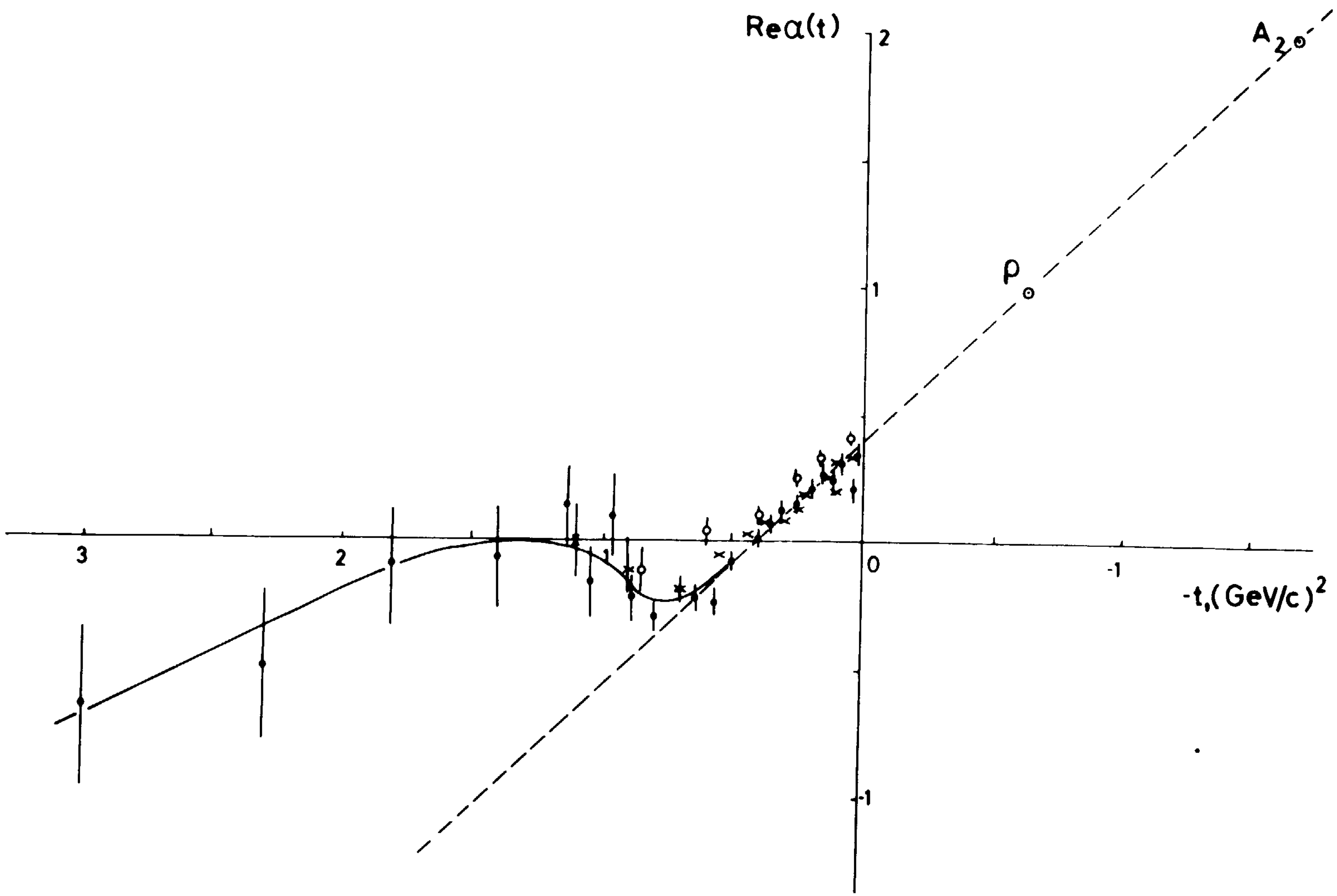

Fig. 10

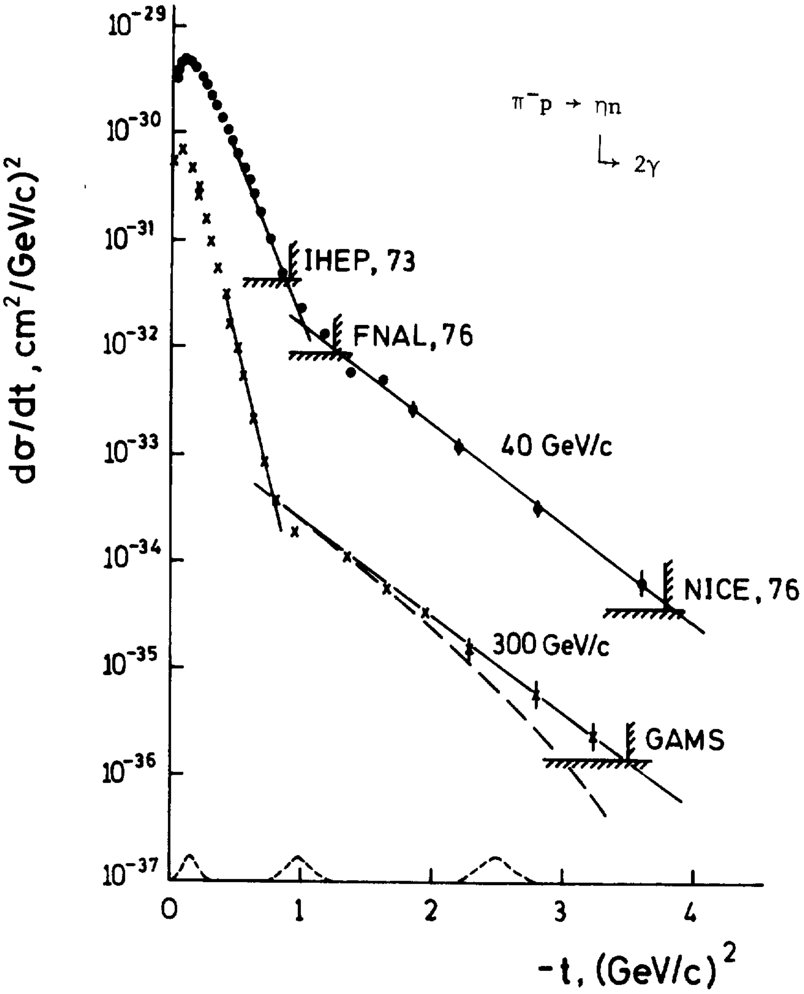

10^{-29}
10^{-30}
10^{-31}
10^{-32}
10^{-33}
10^{-34}
10^{-35}
10^{-36}
10^{-37}
$d\sigma/dt$, $cm^2/(GeV/c)^2$
$\pi^- p \to \eta n$
$\hookrightarrow 2\gamma$
IHEP, 73
FNAL, 76
40 GeV/c
NICE, 76
300 GeV/c
GAMS
0
1
2
3
4
$-t$, $(GeV/c)^2$

Fig. 11

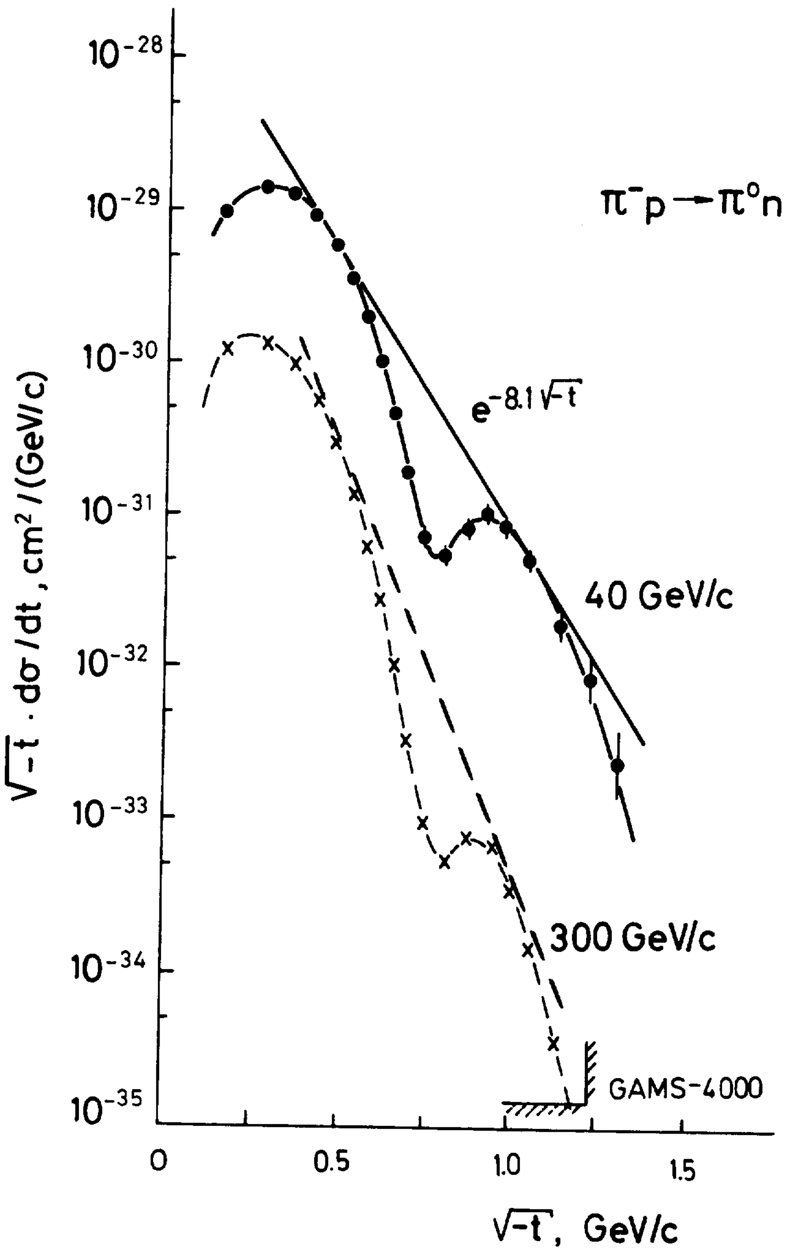
$\pi^- p \rightarrow \pi^0 n$
$e^{-8.1\sqrt{-t}}$
40 GeV/c
300 GeV/c
GAMS-4000
10^{-28}
10^{-29}
10^{-30}
10^{-31}
10^{-32}
10^{-33}
10^{-34}
10^{-35}
0
0.5
1.0
1.5
$\sqrt{-t} \cdot d\sigma/dt$, $cm^2/(GeV/c)$
$\sqrt{-t}$, GeV/c

Fig. 12

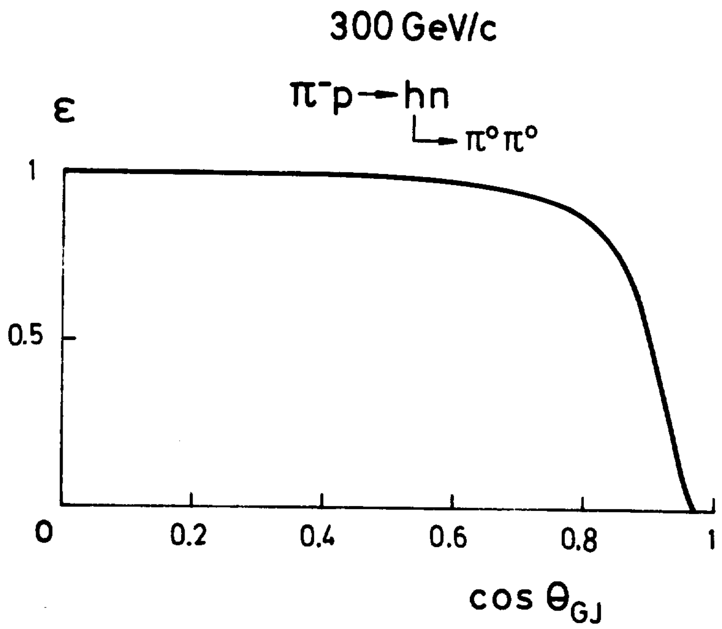
300 GeV/c
$\pi^- p \rightarrow h n$
$\pi^0 \pi^0$
ε
1
0.5
0
0.2
0.4
0.6
0.8
1
cos θ_{GJ}

Fig. 13

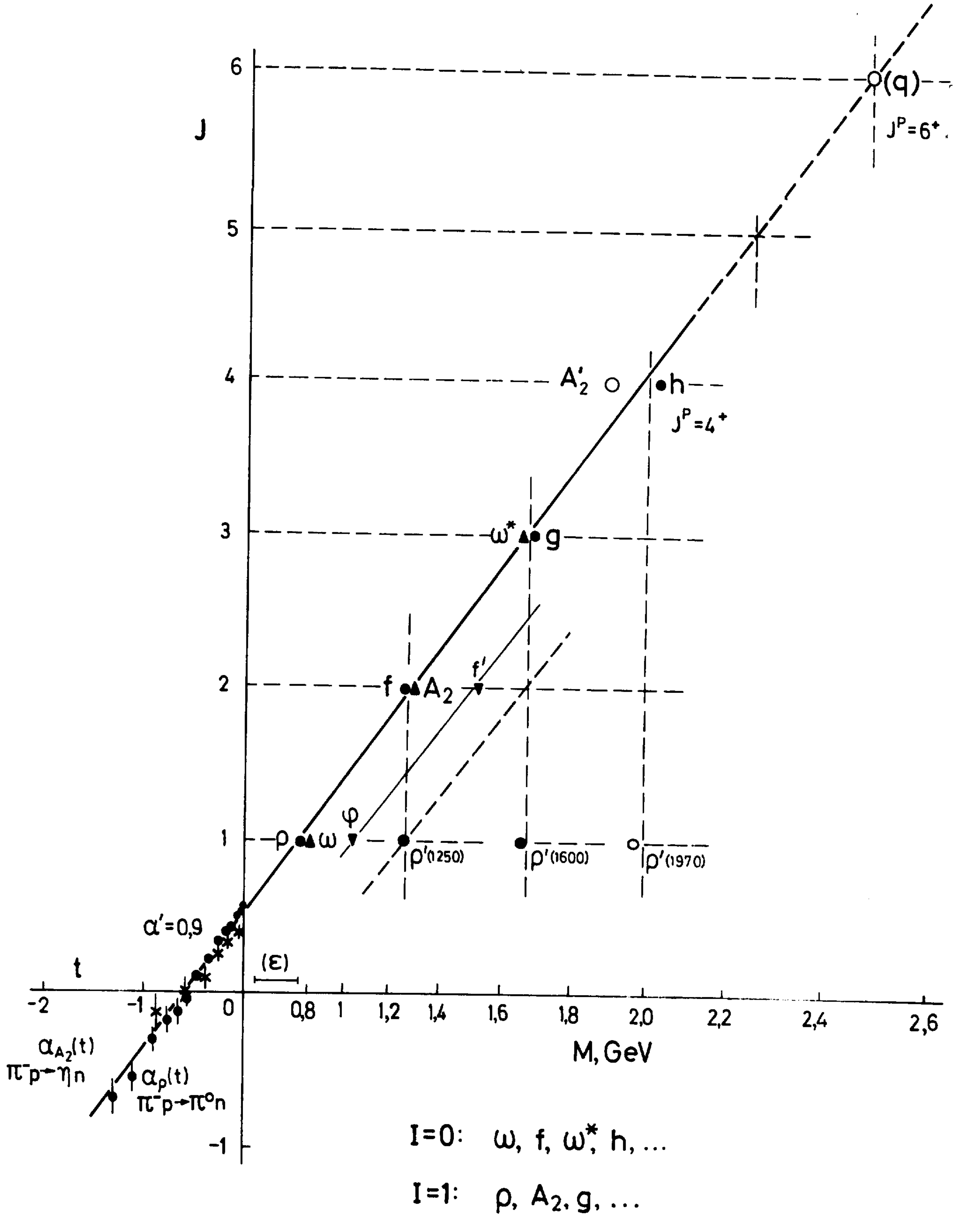
J
6
5
4
3
2
1
-1
(q)
J^P=6+
A'2
h
J^P=4+
ω*
g
f
A2
f'
ρ
ω
φ
ρ'(1250)
ρ'(1600)
ρ'(1970)
α'=0,9
t
(ε)
-2
-1
0
0,8
1
1,2
1,4
1,6
1,8
2,0
2,2
2,4
2,6
M, GeV
α_A2(t)
π⁻p→ηn
α_ρ(t)
π⁻p→π°n
I=0: ω, f, ω*, h, ...
I=1: ρ, A2, g, ...

Fig. 14

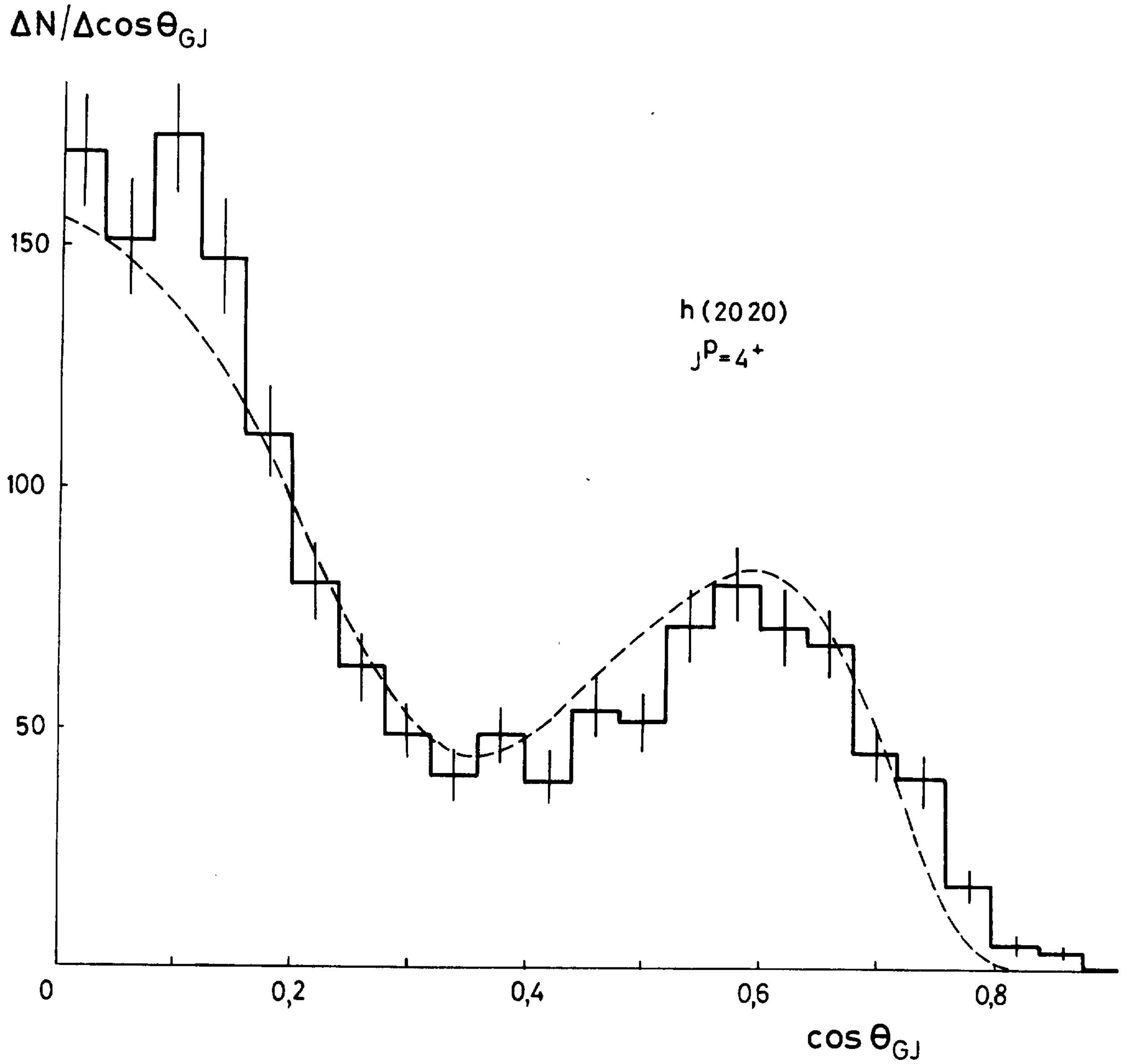

Fig. 15

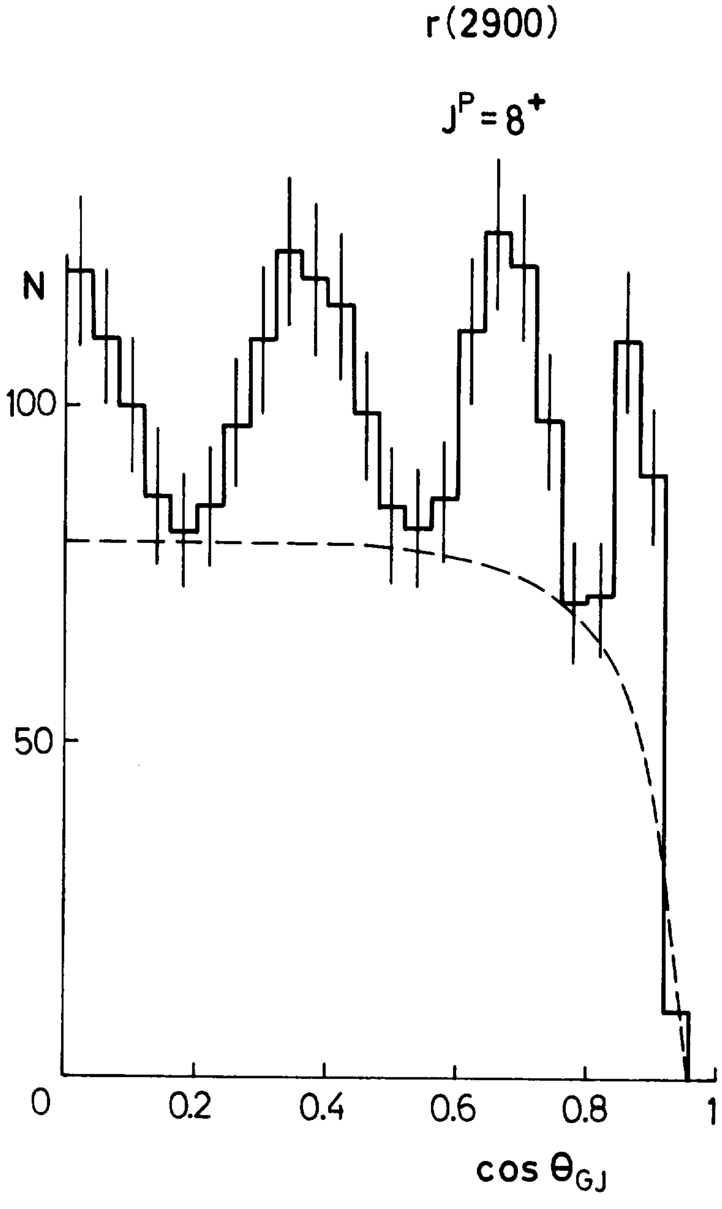

Fig. 16

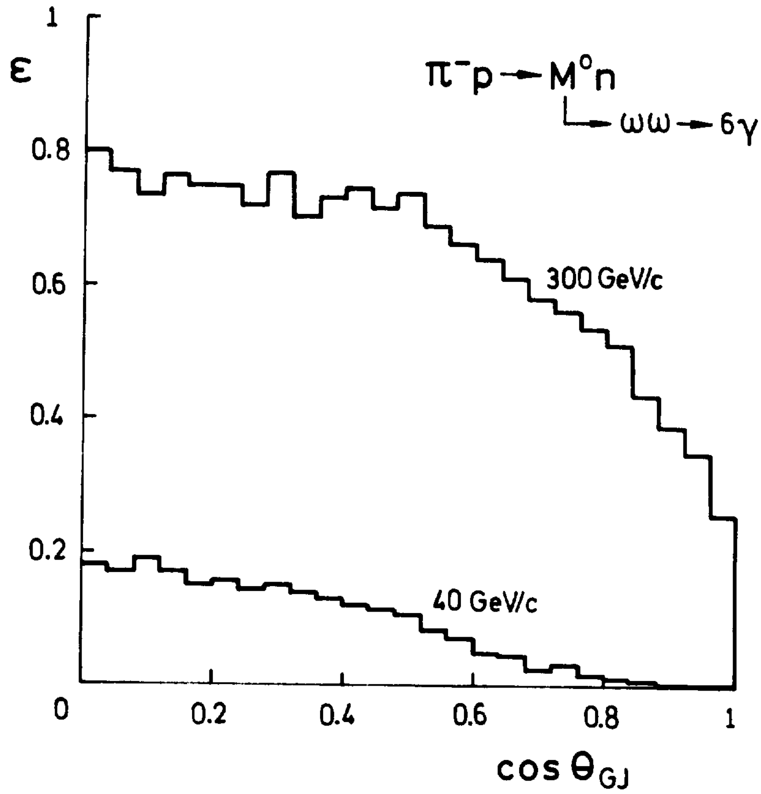

1
ε
$\pi^- p \to M^0 n$
$\omega\omega \to 6\gamma$
0.8
0.6
0.4
0.2
300 GeV/c
40 GeV/c
0
0.2
0.4
0.6
0.8
1
$\cos\theta_{GJ}$

Fig. 17

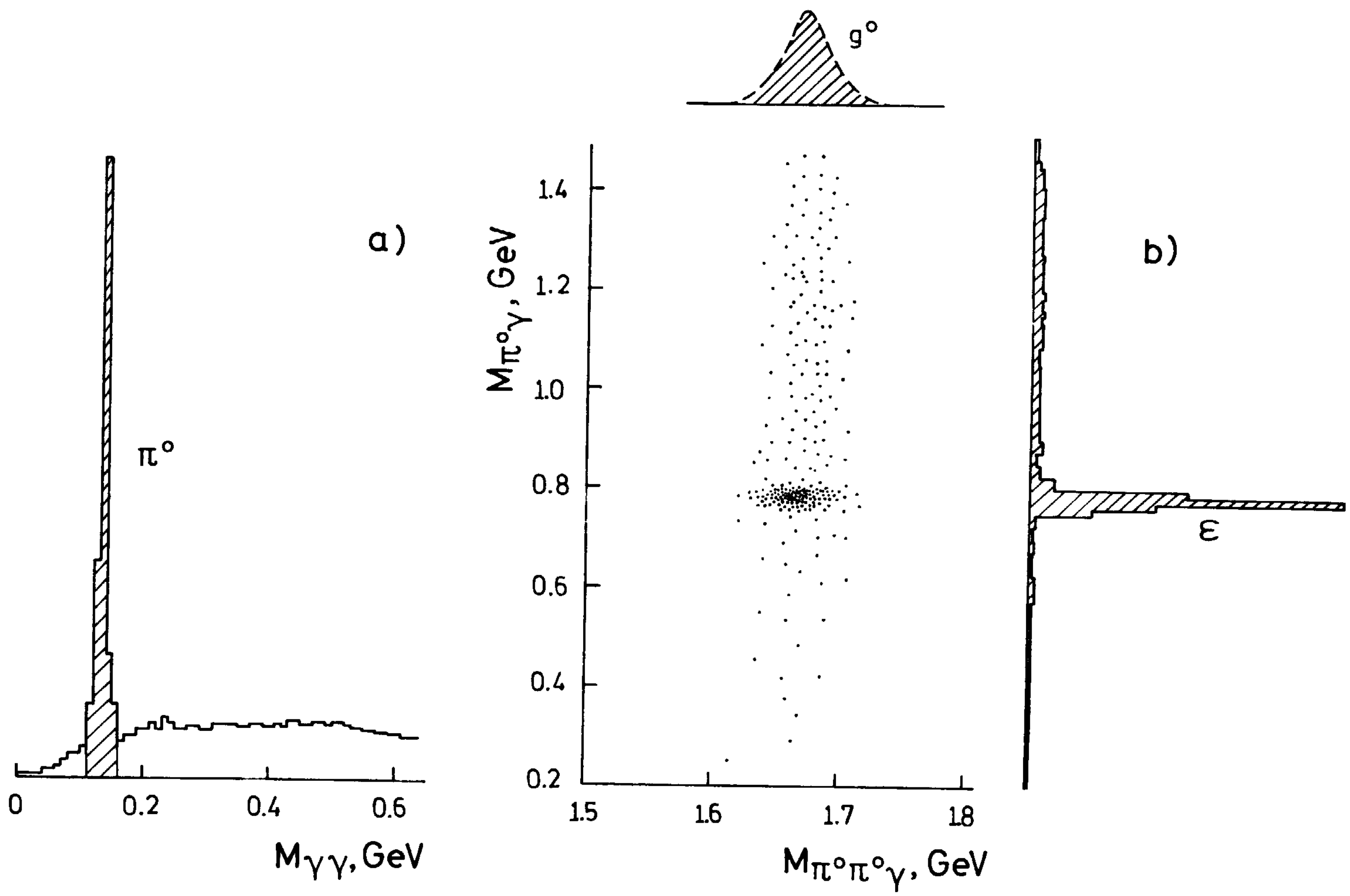
a)
π°
0
0.2
0.4
0.6
Mγγ, GeV
g°
Mπ°γ, GeV
1.4
1.2
1.0
0.8
0.6
0.4
0.2
1.5
1.6
1.7
1.8
Mπ°π°γ, GeV
b)
ε

Fig. 18

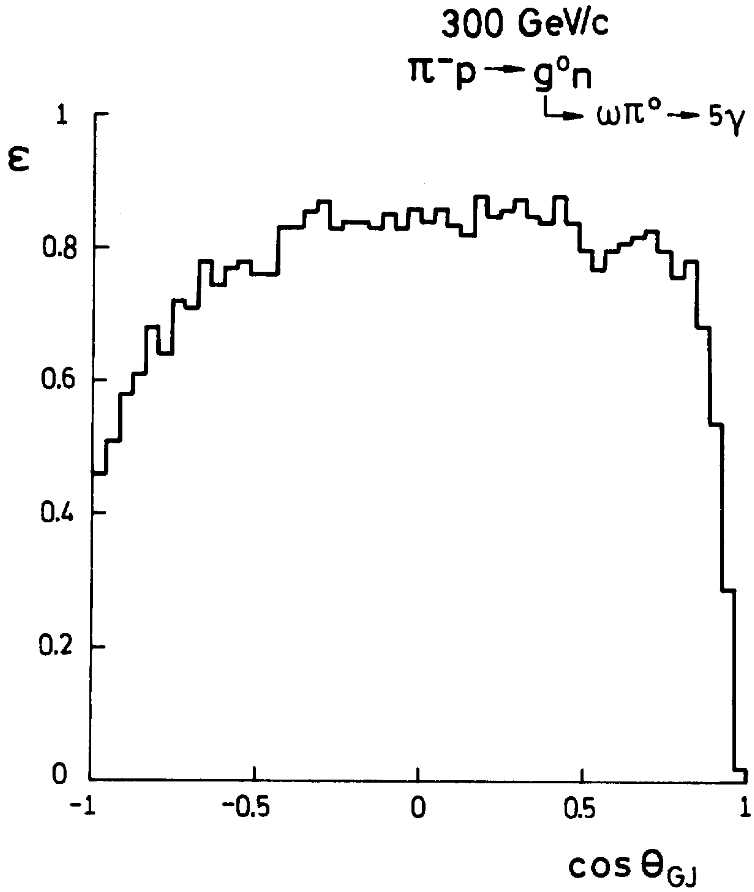
300 GeV/c
$\pi^- p \rightarrow g^0 n$
$\omega\pi^0 \rightarrow 5\gamma$
ε
1
0.8
0.6
0.4
0.2
0
-1
-0.5
0
0.5
1
$\cos\theta_{GJ}$

Fig. 19